Updated global bounds on non-unitarity and heavy neutrinos

Mattias Blennow,[a] Enrique Fernández-Martínez,[b] Josu Hernández-García,[c] Jacobo López-Pavón,[d] Xabier Marcano[b,*] and Daniel Naredo-Tuero[b]

[a] *Department of Physics, School of Engineering Sciences, KTH Royal Institute of Technology,*
  AlbaNova University Center, Roslagstullsbacken 21, SE-106 91 Stockholm, Sweden

[b] *Departamento de Física Teórica and Instituto de Física Teórica UAM/CSIC,*
  Universidad Autónoma de Madrid, Cantoblanco, 28049 Madrid, Spain

[c] *Institute for Theoretical Physics, ELTE Eötvös Loránd University,*
  Pázmány Péter sétány 1/A, H-1117 Budapest, Hungary

[d] *Instituto de Física Corpuscular, Universidad de Valencia and CSIC*
  Edificio Institutos Investigación, Catedrático José Beltrán 2, 46980 Spain

E-mail: emb@kth.se, enrique.fernandez-martinez@uam.es,
garcia.josu.hernandez@ttk.elte.hu, jacobo.lopez@uv.es,
xabier.marcano@uam.es, daniel.naredo@uam.es

We present an updated and improved global fit analysis of current flavor and electroweak precision observables to derive bounds on unitarity deviations of the leptonic mixing matrix and on the mixing of heavy neutrinos with the active flavours, which is motivated by the latest experimental updates on key observables such as V_{ud}, the Z invisible width and the W mass.

The European Physical Society Conference on High Energy Physics (EPS-HEP2023)
21-25 August 2023
Hamburg, Germany

---

*Speaker

1. Introduction and Motivation

Adding right-handed (RH) neutrinos to the Standard Model (SM) particle spectrum is one of the best motivated extensions to address several of the open problems in particle physics. If their mass is above the experimental energy, the RH neutrinos cannot be produced, but their existence induces deviations from unitarity of the leptonic mixing matrix [1], so they can still be probed for at the intensity frontier via electroweak precision observables (EWPO), universality ratios or charged lepton flavor violating (cLFV) processes.

Upon integrating them out, such heavy RH neutrinos induce light neutrino masses via the dim-5 Weinberg operator,

$$m_\nu = -\Theta M_M \Theta^T \,, \tag{1}$$

where Θ is the mixing between the active SM neutrinos and the RH ones, given as the ratio between their Dirac and Majorana mass matrices, $\Theta \equiv m_D M_M^{-1}$. At dimension 6, the only operator generated at tree level induces the aforementioned deviations from unitarity of the leptonic mixing matrix N.

A completely general way to parametrize unitarity deviations is through a small Hermitian matrix η [2]:

$$N = (\mathbb{I} - \eta)\, U \,, \tag{2}$$

where U is the unitary matrix that diagonalizes the Weinberg operator. This parametrization is convenient as it encodes non-unitarity effects regardless of the UV completion that originates the deviations and how many fields it contains. In the particular case of heavy RH neutrinos, η corresponds to (half of) the coefficient of the dim-6 operator obtained upon integrating them out:

$$\eta = \frac{1}{2}\Theta\Theta^\dagger \,. \tag{3}$$

Here we present an updated and improved global fit analysis of an extended set of observables that are affected by a non-unitary leptonic mixing matrix. The motivation to update the analysis is driven by new experimental results on key observables such as V_{ud}, the Z invisible width and the W boson mass, although we also improve the robustness of the analysis and extend it to new scenarios. Our analysis provides upper limits on non-unitarity effects encoded by η or, equivalently, on the mixings between RH neutrinos and active ones, the strongest bounds for heavy neutrinos above the EW scale. These results correspond to the analysis in Ref. [3], where all the details can be found.

2. Scenarios under study

In all generality, the dim-5 and 6 operators are independent, meaning that in the most general case we can decouple η from light neutrino masses and mixings. Nevertheless, in models with not many heavy neutrinos and thus less freedom, it is possible to find correlations between them. In order to cover from the minimal to the most general case, we consider the following scenarios:

- **2N-SS**: The minimal scenario that accommodates oscillation data adding only 2 RH neutrinos. Here the dim-5 and 6 operators are fully correlated, since the latter (and thus η) can be fully reconstructed from the former up to a global scale [4].

- **3N-SS**: The next-to-minimal scenario with 3 RH neutrinos, where the dim-5 operator still imposes strong correlations on η [5].

- **G-SS**: The most general RH neutrino scenario where we assume a general η matrix, independent of neutrino oscillation data, which encodes the low-energy effects of an arbitrary number of heavy RH neutrinos.

All these RH neutrino scenarios induce a η-matrix that is positive-definite and, consequently, it has to fulfill the Schwarz inequality:

$$\left|\eta_{\alpha\beta}\right| \leq \sqrt{\eta_{\alpha\alpha}\eta_{\beta\beta}}, \tag{4}$$

which is actually saturated in the minimal scenarios 2N-SS and 3N-SS. A complete general scenario with generic deviations from unitarity not requiring η to be positive-definite or subject to the Schwarz inequality was also studied in [3], although we do not report the results here for brevity.

3. Observables and details of the analysis

The global analysis presented here consisted in a fit to the following set of flavor and electroweak precision observables:

- Four determinations of the W-boson mass by LEP, Tevatron, LHCb and ATLAS. We do not include the CDF-II result since, in this context of unitarity deviations, it is in more than 5σ tension with other EWPO [3].

- Two determinations of the effective weak angle by LHC and Tevatron.

- Five LEP observables measured at the Z-pole (Γ_Z, $\sigma^0_{\rm had}$, R_e, R_μ, R_τ), and a determination of the Z invisible width from CMS.

- Five weak decay ratios constraining lepton flavor universality: $R^\pi_{\mu e}$, $R^\pi_{\tau\mu}$, $R^K_{\mu e}$, $R^\tau_{\mu e}$, $R^\tau_{\tau\mu}$.

- Ten weak decays constraining CKM unitarity, whose first raw currently lies below 1 at the 2-3σ level (the so-called Cabibbo anlge anomaly).

- cLFV observables, which constrain the off-diagonal entries of η in general, but also the diagonal entries in the 2N-SS and 3N-SS due to the saturation of the Schwarz inequality.

Compared to previous analyses [6–8], we update and complete the list of observables, with a better handle of the correlations; we improve the statistical treatment with an explicit calibration of the test statistic; and we improve the analysis by making consistent predictions for our input observables rather than using the values provided in the PDG, which are already obtained from a global fit to precision data. Moreover, we extend the number of scenarios, as the 2N-SS was missing. All these details of the analysis, as well as the explicit dependences of the observables on the non-unitarity effects, can be found in Ref. [3].

95% CL	2N-SS		3N-SS		G-SS
	NO	**IO**	**NO**	**IO**	
η_{ee}	$9.4 \cdot 10^{-6}$	$5.5 \cdot 10^{-4}$	$1.3 \cdot 10^{-3}$	$1.4 \cdot 10^{-3}$	$[0.081, 1.4] \cdot 10^{-3}$
$\eta_{\mu\mu}$	$1.3 \cdot 10^{-4}$	$3.2 \cdot 10^{-5}$	$1.1 \cdot 10^{-5}$	$1.0 \cdot 10^{-5}$	$1.4 \cdot 10^{-4}$
$\eta_{\tau\tau}$	$2.1 \cdot 10^{-4}$	$4.5 \cdot 10^{-5}$	$1.0 \cdot 10^{-3}$	$8.1 \cdot 10^{-4}$	$8.9 \cdot 10^{-4}$
$\text{Tr}\,[\eta]$	$2.9 \cdot 10^{-4}$	$6.0 \cdot 10^{-4}$	$1.9 \cdot 10^{-3}$	$1.5 \cdot 10^{-3}$	$2.1 \cdot 10^{-3}$
$|\eta_{e\mu}|$	$1.2 \cdot 10^{-5}$	$1.3 \cdot 10^{-5}$	$1.2 \cdot 10^{-5}$	$1.2 \cdot 10^{-5}$	$1.2 \cdot 10^{-5}$
$|\eta_{e\tau}|$	$2.2 \cdot 10^{-5}$	$1.4 \cdot 10^{-4}$	$9.0 \cdot 10^{-4}$	$8.0 \cdot 10^{-4}$	$8.8 \cdot 10^{-4}$
$|\eta_{\mu\tau}|$	$1.3 \cdot 10^{-4}$	$3.5 \cdot 10^{-5}$	$5.7 \cdot 10^{-5}$	$1.8 \cdot 10^{-5}$	$1.8 \cdot 10^{-4}$

Table 1: 95% CL upper bounds (or preferred intervals) for the non-unitarity matrix η in the 3 scenarios considered here: the minimal scenario with 2 RH neutrinos (2N-SS), the next-to-minimal with 3 RH neutrinos (3N-SS) and the general scenario with an arbitrary number of RH neutrinos (G-SS). These results can be also understood as bounds on the total (squared) mixings of the RH neutrinos to a given flavor, and easily translated to the α-parametrization (see Ref. [3] for the explicit relations).

4. Results and discussion

The final results of our analysis are collected in Table 1, given as upper limits on the elements of η, as well as on its trace, included as a measurement of the *total* deviation from unitarity regardless of its particular flavor structure. They are obtained from the global fit described in the previous sections and imposing the Schwarz inequality, with the only exception of $\eta_{e\mu}$ in the G-SS, for which the strongest bounds actually arise from μ-e transitions. Notice that we provide here only the 95%CL upper bounds for brevity, nevertheless these cannot be naively scaled to other confidence levels as the results do not follow Wilks' theorem and the resulting profiles are not gaussian. The relevant profiles for this task are given in Ref. [3].

In order to understand these results, it is interesting to first analyze the overall preference of the data. On the one hand, M_W and s_w^2 show a mild, about 1σ, preference for a non-zero $\eta_{ee} + \eta_{\mu\mu}$, and similarly the LFU ratios moderately prefer that $\eta_{ee} > \eta_{\mu\mu}$, also around 1σ. On the other hand, the CKM data strongly disfavors non-zero values of $\eta_{\mu\mu}$, as they can only worsen the Cabibbo anomaly, and the strong cLFV bounds on the μ-e sector require either the electron or the muon mixing to be very small. Combining all these aspects, together with the lack of preference for a non-zero $\eta_{\tau\tau}$, we conclude that the data prefers a non-zero η_{ee} with suppressed $\eta_{\mu\mu}$ and $\eta_{\tau\tau}$.

This data-preferred structure is represented with a black star in Fig. 1, where we also display the flavor patterns for the different scenarios we studied and for both normal and inverted orderings. Comparing the mixing pattern in each scenario with the preference of the data, we can understand the general behavior of our results.

In the case of the minimal 2N-SS scenario, the flavor structure is very restricted as a result of the strong correlations between the dim-5 and 6 operators, and thus the regions are smaller and very different in both orderings. In particular, the normal ordering (NO) requires a suppressed
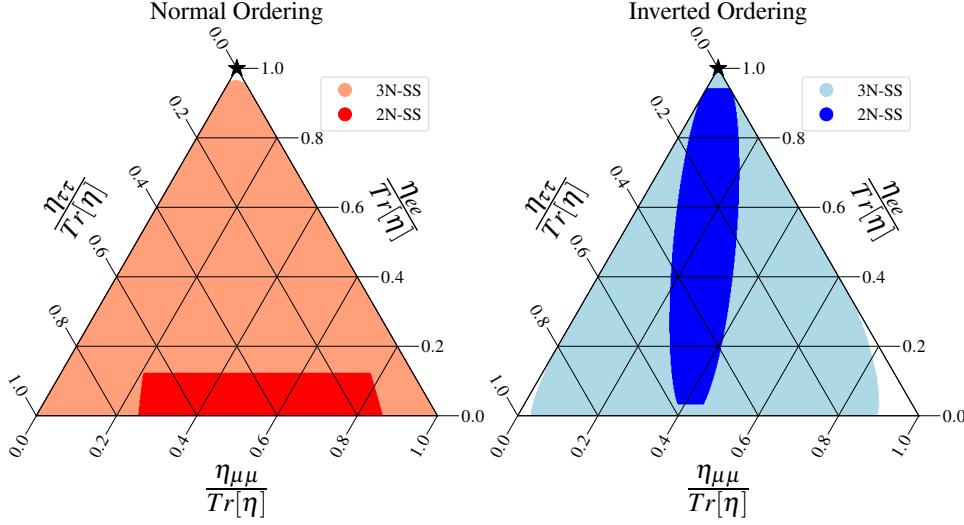
Figure 1: Regions in the RH neutrino mixing flavor space consistent with current neutrino oscillation data for both normal and inverted orderings. Darker regions correspond to the minimal 2N-SS scenario, while lighter ones to the next-to-minimal 3N-SS case. The whole triangle is available in the general G-SS scenario. The black star indicates the preference of the data.

mixing to electrons with respect to other flavors, which is precisely the opposite of what the data prefers. Therefore, this scenario cannot accommodate this preference and it leads to strong bounds, specially on η_{ee}. On the contrary, an inverted ordering (IO) allows for mixing patterns closer to that preferred by the data, and thus the bounds on η_{ee} are relaxed.

Despite of these differences between the two orderings, the bounds in the 2N-SS are in general stronger than for other scenarios. The reason is the saturation of the Schwarz inequality in Eq. (4), which introduces the cLFV observables into the fit. Consequently, the strong bounds on μ-e transitions impose severe constraints also for the diagonal elements of η, in particular in for the IO, where it is not possible to suppress η_{ee} nor $\eta_{\mu\mu}$ to avoid this bound.

Moving into the 3N-SS case, the additional freedom enlarges the allowed regions in the mixing flavor space, as can be seen in Fig. 1, so they get closer to the data-preferred pattern in both orderings. Moreover, they also allow for suppressed mixings to either electrons or muons, so the bounds from μ-e transitions can be easier fulfilled. Consequently, the constraints are relaxed with respect to the 2N-SS, with the exception of $\eta_{\mu\mu}$ and $\eta_{e\mu}$, which are still very constrained by the Cabibbo anomaly and μ-e transitions, respectively.

Finally, in the general case η can be decoupled from oscillation data and therefore the whole triangle is allowed. In particular, the pattern with mixings only to electrons becomes available, relaxing the constraints further and even showing a slight preference ($\approx 2\sigma$) for a non-zero value of η_{ee}. Moreover, in this G-SS case the Schwarz inequality is not saturated, meaning that cLFV observables constrain only the off-diagonal elements and are thus not included into the global fit. Nevertheless, this inequality does translate the global bounds on the diagonal elements into off-diagonal ones, which provides stronger bounds for $\eta_{e\tau}$ and $\eta_{\mu\tau}$ than the associated cLFV observables. In the case of $\eta_{e\mu}$, it is still better constraint by μ-e transitions, so the bound is basically the same in all scenarios.

5. Conclusions

We have updated and improved upon present constraints on the unitarity of the leptonic mixing matrix and the mixing of heavy right-handed neutrinos with the SM active flavors. Our global fit to flavor and electroweak precision observables leads to constraints on all the η parameters ranging between 10^{-3} and 10^{-5} at 2σ, with the exception of a preference for non-unitarity at the level of $\eta_{ee} \sim 10^{-3}$ at around 2σ for the general case. The latter translates to a mixing to heavy neutrinos with the electron at the $|\theta_e| \sim 10^{-2}$ level.

Our analysis provides the strongest bounds for RH neutrinos heavier than the EW scale, and they are valid as long as the new degrees of freedom are heavier than the mass of the Z. For lighter new particles, some of the LEP constraints at the Z pole are lost, but the remaining observables apply down to the mass of the τ, where direct searches for RH neutrinos provide better sensitivities. Notice also that our treatment of the cLFV was conservative, and that for very heavy masses they could be even stronger bounds, which would need to be checked for each particular model [3].

References

[1] A. Broncano, M. B. Gavela and E. E. Jenkins, Phys. Lett. B **552** (2003), 177-184 [erratum: Phys. Lett. B **636** (2006), 332] [arXiv:hep-ph/0210271].

[2] E. Fernandez-Martinez *et al.* Phys. Lett. B **649** (2007), 427-435 [arXiv:hep-ph/0703098].

[3] M. Blennow, E. Fernández-Martínez, J. Hernández-García, J. López-Pavón, X. Marcano and D. Naredo-Tuero, JHEP **08** (2023), 030 [arXiv:2306.01040].

[4] M. B. Gavela *et al.* JHEP **09** (2009), 038 [arXiv:0906.1461].

[5] E. Fernandez-Martinez *et al.* JHEP **10** (2015), 130 [arXiv:1508.03051].

[6] S. Antusch and O. Fischer, JHEP **10** (2014), 094 [arXiv:1407.6607].

[7] E. Fernandez-Martinez *et al.* JHEP **08** (2016), 033 [arXiv:1605.08774].

[8] M. Chrzaszcz *et al.* Eur. Phys. J. C **80** (2020) no.6, 569 [arXiv:1908.02302].